and this sensation persisted for 7 or 8 seconds in the phantom. (vi) Reorganization was relatively rapid. In one patient, our study was carried out 4 weeks after limb amputation rather than 12 years.

That patients "refer" paresthesiae to a "phantom limb" is in itself not new. We have attempted to systematically relate such findings to studies of animal physiology (*1*, *4*). For example, we suggest that the reason we found two clusters of reference fields exhibiting topography—one on the face and one near the amputation line—is because the hand area in Penfield's homunculus (in the somatosensory cortex) is flanked on one side by the face and on the other side by areas around the line of amputation (for example the upper arm and shoulder). We would therefore expect sensory input from both these regions to "invade" the cortical hand area and provide a basis for referred sensations.

The very existence of phantom limbs might be partially explained by our hypothesis. If tactile and proprioceptive input from surrounding tissue "takes over" the brain areas corresponding to the amputated limb, spontaneous discharges arising from neurons innervating these tissues would be misinterpreted as arising from the missing limb. This hypothesis is different from, although not incompatible with, the idea that phantom limbs result from the persistence of a "neurosignature" in a diffuse neuronal pool (*5*). Our observation that the changes can occur as early as 4 weeks after amputation is especially interesting since it suggests that the reorganization is a result of the unmasking of "silent" synapses rather than of anatomical changes such as "sprouting." Perhaps, even in normal adults, input from the face projects simultaneously to both face and hand areas in the cortex or thalamus (and input from the hand to both hand and face areas). The unwanted input to the hand area, however, may be subject to tonic inhibition (for example, through an inhibitory interneuron) by the "correct" axon carrying a signal from the hand. When an arm is amputated, this occult input is unmasked through disinhibition. It remains to be seen whether this unmasking is permanent or whether the patients eventually begin to "ignore" the referred sensations.

Whatever the ultimate interpretation may be, however, our findings suggest that the adult mammalian brain has a latent capacity for much more rapid functional reorganization over a much greater area than previously thought, a capacity that could conceivably be exploited for therapeutic purposes.

V. S. Ramachandran
D. Rogers-Ramachandran
M. Stewart
Brain and Perception Laboratory, Department of Psychology, University of California, San Diego, La Jolla, CA 92093–0109

REFERENCES

1. T. P. Pons *et al.*, *Science* **252**, 1857 (1991).
2. V. S. Ramachandran, M. Stewart, D. C. Rogers-Ramachandran, *Neuroreport* **3**, 583 (1992).
3. ———, *Soc. Neurosci. Abstr.*, in press.
4. M. M. Merzenich *et al.*, *J. Comp. Neurol.* **224**, 591 (1984); P. Wall, *Philos. Trans. R. Soc. London Ser. B* **278**, 361 (1977).
5. R. Melzack, *Sci. Am.* **266**, 120 (April 1992).
7. We thank patients V.Q., W.K., and D.W. for their cooperation; M. Botte and R. Abrams for referring them to us; M. Parsa and O. Gil for assistance; and the Air Force Office of Scientific Research and the Office of Naval Research for support.

27 May 1992; accepted 1 September 1992

Response: The preliminary observations of Ramachandran *et al.* are remarkable for they not only suggest that areas of the brain that undergo reorganization after peripheral or central damage are capable of mediating tactile perception, but also that central mechanisms alone can be responsible for sensations in phantom limbs.

It has often been suggested that incidental stimulation of neuromas immediately adjacent to an amputated region is responsible for phantom sensations in a missing limb. Generally, representations of adjacent body parts are located in adjacent regions of cortex. Ramachandran *et al.* have taken advantage of the fact that the cortical representation of the face is not adjacent to representations of adjacent body parts, but is instead adjacent to the representation of the upper limb. They were thus able to dissociate the effects of stimulating neuromas, which are located at the end of an amputation, from those of stimulating the adjacent cortical body representation. Stimulation of neuromas was clearly not necessary for the perception of phantom sensations, but activation of cortex that had reorganized to respond to inputs from the face was apparently sufficient for such perception.

The mechanism by which such reorganization of the brain takes place is not yet clear. With regard to the rapidity of the phantom limb being activated by touching the face, I agree with Ramachandran *et al.* that sprouting of new inputs seems unlikely, but an unmasking of preexisting inputs also seems unlikely because anatomical studies have repeatedly demonstrated that areas of cortex representing the hand do not receive connections from regions of the brain representing the face. Whatever mechanism is ultimately found to be responsible for the reorganization, Ramachandran *et al.* have made an enormous contribution by showing that such reorganized cortex is capable of processing sensory inputs so that they result in tactile perception.

Tim P. Pons
Laboratory of Neuropsychology, National Institute of Mental Health, Bethesda, MD 20892

21 July 1992; accepted 1 September 1992

Structural Similarity Between Transforming Growth Factor–β2 and Nerve Growth Factor

The crystallographic determination of transforming growth factor–β2 (TGF-β) reported by S. Daopin *et al.* (*1*) offers an exciting insight into the structures adopted by this superfamily. However, the fold may not be as unusual as first anticipated. I have analyzed the major details of this topology and have found them to be remarkably consistent with the structure of nerve growth factor (NGF) that was published last year by N. Q. McDonald *et al.* (*2*).

The most obvious global similarities between the two structures are, first, the long looping antiparallel strands that lead to the unusual absence of a traditional hydrophobic core and, second, their homodimeric form. In addition, the strict conservation of nine cysteines per monomer reported for the TGF-β family is mirrored by an equally important set of six cysteines in NGF. All six cysteines from NGF appear to have equivalent sequential and structural locations in TGF-β and form their disulfide bonds with equivalent partners (Fig. 1).

A major structural difference between these proteins is the absence, in NGF, of three helices and three disulfide-forming cysteine residues. These differences are particularly significant, as they are interdependent. The extra intrasubunit disulfide bond in TGF-β forms a bridge between helix α1 and strand β1 and seems to be vital for amino-terminal stabilization (Fig. 1). As this helix is absent in NGF, the extra disulfide is not required. The remaining cysteine, which forms an intersubunit disulfide in TGF-β, is absent in NGF and will probably reflect the different packing arrangements adopted by each homodimer.

The absence of all three helices in NGF would appear to be of only peripheral importance to the core topology, as they are all located in, or near, loop regions. Similar insertions and deletions have been observed in other topologies with low sequence identities, such as plastocyanin (*3*) and azurin (*4*), where they also have little effect on the overall fold.

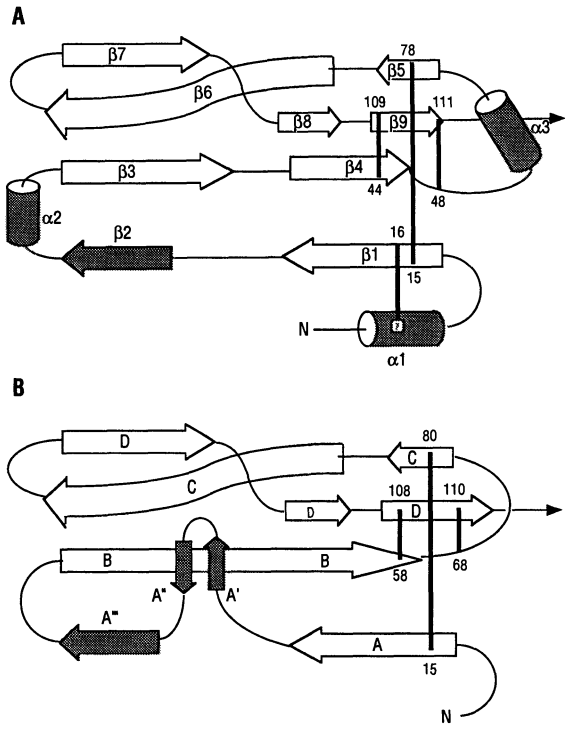

Fig. 1. Schematic representations of (**A**) TGF-β and (**B**) NGF, highlighting the overall similarities in topology. Secondary structure and residue numbering systems are taken from the original references. The α helices are represented by cylinders, and β strands are drawn as arrows. Cysteine residues that form intrasubunit disulfide bonds are numbered, and their bonds are represented by bold lines. N represents the amino terminal. The extra TGF-β disulfide bond is located between residues 7 and 16. Regions of regular secondary structure that are not present in both proteins are shaded. These include all of the helices from TGF-β, as well as strands A′ and A″ from NGF. Strands A‴ in NGF and β2 in TGF-β are probably not superimposable in three dimensions.

Despite these structural similarities, there is almost no sequence identity between the two proteins. The only conserved features are the disulfide bonding patterns, which appear to play a dominant role in the absence of a significant hydrophobic core. Detailed structural comparisons and superpositions should provide rewarding results, particularly as a reliable sequence alignment could be derived. It would appear that this fold, far from being unique, may well provide the framework on which many proteins are based. If so, this will be an unexpected bonus provided by an already intriguing structure.

Mark B. Swindells
Protein Engineering Research Institute, 6-2-3 Furuedai, Suita, Osaka 565, Japan

REFERENCES

1. S. Daopin, K. A. Piez, Y. Ogawa, D. R. Davies, *Science* **257**, 369 (1992).
2. N. Q. McDonald *et al.*, *Nature* **354**, 411 (1991).
3. T. P. J. Garrett, D. J. Clingeleffer, J. M. Guss, S. J. Rogers, M. C. Freeman, *J. Biol. Chem.* **259**, 2822 (1984).
4. E. T. Adman and L. H. Jensen, *Isr. J. Chem.* **21**, 8 (1981).

31 July 1992; accepted 9 September 1992

Response: The observation by Swindells, as well as by A. G. Murzin and C. Chothia (*1*), that TGF-β2 and NGF are topologically similar is interesting, particularly in view of the low sequence homology and the absence of the three helices in the NGF. In order to obtain a more detailed comparison, we have compared the three-dimensional (3-D) structures of the two proteins (*2–4*) using the program ALIGN (*5*) (Fig. 1). The results confirm that although the two structures are not similar in detail, there is a general topological similarity. Out of about 110 residues in the two structures, 73 pairs of α carbons have been aligned within 10 Å of each other with a root-mean-square (rms) deviation of 3.3 Å. This alignment defines the most similar part of the two structures, consisting of the β-sheet regions of the four fingers of TGF-β2 [β-sheet strands A, B, C, and D in NGF (*4*)] and the three disulfide bridges at the base of the fingers. These finger strands not only have similar lengths but also have similar twists, including a right-handed crossover twist in the fourth strand that is found in both structures at the same location. As a control, the variable regions of immunoglobulin light chain domains of McPC603 and J539 were aligned and gave an rms deviation of 0.86 Å for 103 Cα pairs.

This general topological similarity between the two growth factors is unexpected, as there is only an 11% sequence identity between them (the two immunoglobulins have a 55% sequence identity) (Fig. 2). Six of the eight identical amino acid pairs, however, are the cysteines of the three invariant disulfide bridges, which suggests that these disulfides form a common core arrangement. Alignment of the six cysteines alone yields a rms difference of 0.91 Å.

The remaining 40 residues with poor alignment contain features peculiar to one molecule but not found in the other. For instance, TGF-β2 has three α helices that do not exist in NGF, and NGF has three short β strands between strands A and B that have no counterpart in the TGF-β2 structure.

Both proteins exist as dimers, but the mode of dimer formation is profoundly different. First, the dyad axes relating the two subunits are roughly at right angles, with the dyad in NGF running approximately parallel to the long axis of the subunit, as compared with the TGF-β2 dyad, which is at about 90° to this axis (Fig. 3). This difference in the axes results in a head-to-tail association for TGF-β2 compared with a head-to-head association for NGF. Second, the dimer interface of NGF contains the "back of the hands" compared with the "palms" in TGF-β2. This results in the hydrophobic patches that involve the dimer formation being on the opposite surfaces of the molecule. Third, the TGF-β2 interface involves the longest α helix of one subunit and the β-sheet finger region of the other subunit, whereas in NGF the dimer interface is formed mainly with the residues of the β-sheet region. These differences in dimer formation are further supported by the 3-D–1-D profile analysis of J. U. Bowie

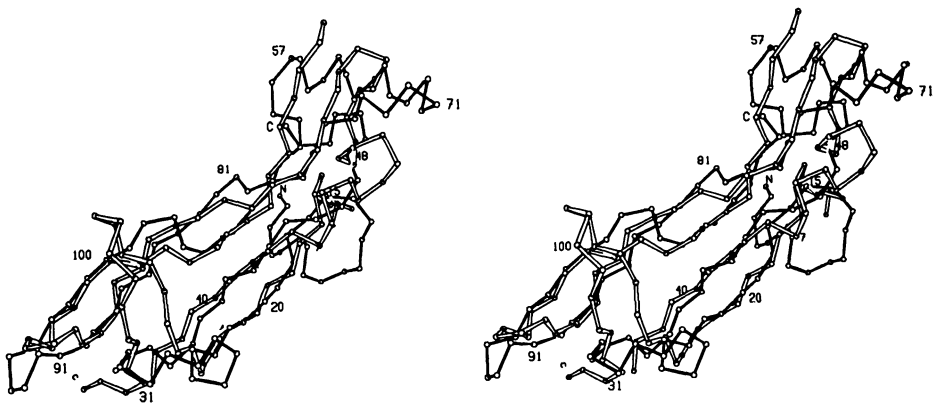

Fig. 1. Stereo drawing of the backbone Cα atoms of TGF-β2 (solid bonds) superimposed onto the Cα's of NGF (open bonds). The residues are labeled with the TGF-β2 numbering. The drawing is made with the program ORTEP (*8*).

Fig. 2. The sequence alignment between TGF-β2 and NGF. The two sequences are aligned according to their structural alignment. The TGF-β2 numbering is used.

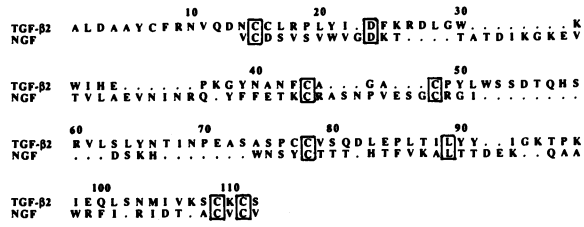

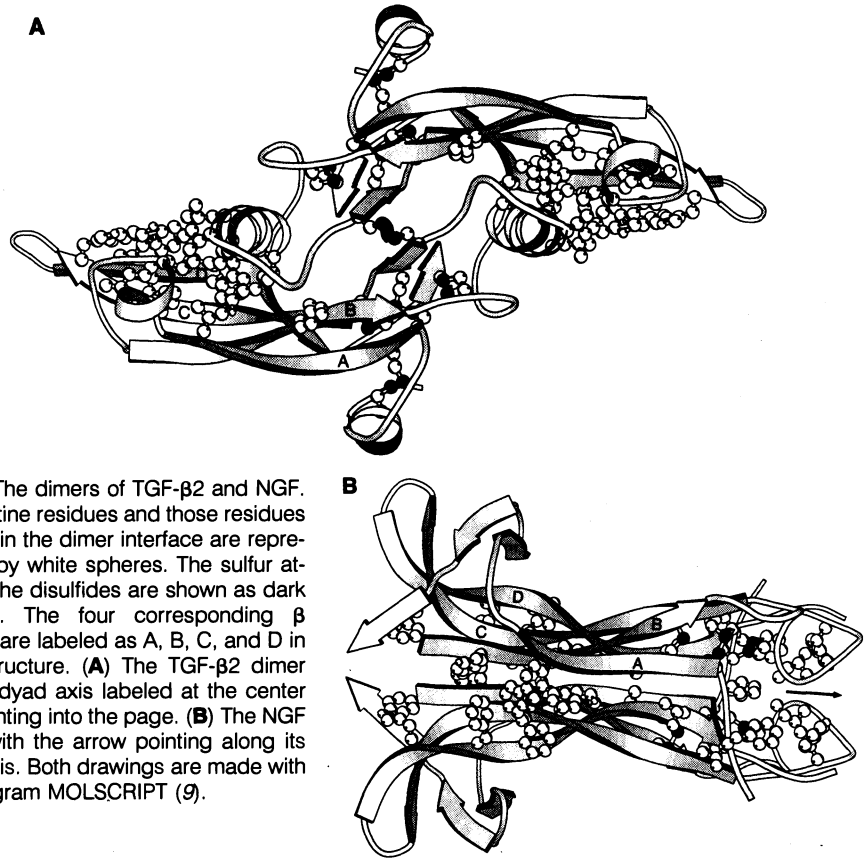

Fig. 3. The dimers of TGF-β2 and NGF. The cystine residues and those residues located in the dimer interface are represented by white spheres. The sulfur atoms of the disulfides are shown as dark spheres. The four corresponding β strands are labeled as A, B, C, and D in each structure. (**A**) The TGF-β2 dimer with its dyad axis labeled at the center and pointing into the page. (**B**) The NGF dimer with the arrow pointing along its dyad axis. Both drawings are made with the program MOLSCRIPT (*9*).

posed type II receptor binding site for TGF-β2 has been localized to the surface residues within the region 40 to 80 (*7*), which is at the back of the heel of the hand. Conversely, the putative receptor binding site for NGF is located around the three–hairpin loop region that includes residues 29 to 35, 43 to 48, and 92 to 98; TGF-β2 lacks two of these loops, 29 to 35 and 43 to 48.

In summary, the topology of the four central β strands together with the three pairs of disulfides is conserved between the TGF-β and NGF families despite the low sequence homology and their very different roles in mediating the dimer formation. These common features may represent a more general structural motif that could be used as a common building block for other cysteine-rich growth factors.

Sun Daopin
Gerson H. Cohen
David Davies
Laboratory of Molecular Biology, National Institute of Diabetes, Digestive, and Kidney Diseases, National Institutes of Health, Bethesda, MD 20892

REFERENCES AND NOTES

1. A. G. Murzin and C. Chothia, *Curr. Opin. Struct. Biol.*, in press.
2. S. Daopin, K. A. Piez, Y. Ogawa, D. R. Davies, *Science* **257**, 369 (1992).
3. M. P. Schlunegger and M. G. Grütter, *Nature* **358**, 430 (1992).
4. N. Q. McDonald *et al.*, *ibid.* **354**, 411 (1991).
5. Y. Satow, G. H. Cohen, E. A. Padlan, D. R. Davies, *J. Mol. Biol.* **190**, 593 (1986).
6. J. U. Bowie, R. Lüthy, D. Eisenberg, *Science* **253**, 164 (1991).
7. S. W. Qian *et al.*, *Proc. Natl. Acad. Sci. U.S.A.* **89**, 6290 (1992).
8. C. K. Johnson, *ORTEP: A Fortran Thermal-Ellipsoid Plot Program For Crystal Structure Illustrations* (Oak Ridge National Laboratory, Oak Ridge, TN, 1970).
9. P. Kraulis, *J. Appl. Cryst.* **24**, 946 (1991).
10. We are grateful to A. Wlodawer for giving us the NGF coordinates used in this comparison.

3 September 1992; accepted 9 September 1992

Silica-Carbonate Isotopic Temperature Calibration

A. Shemesh *et al.* (*1*) use the oxygen isotope fractionation between biogenic silica and foraminiferal carbonate in deep-sea sediments to determine variations in both the temperature of deposition and the isotopic composition of seawater over the last glacial cycle. It appears that they have overestimated the sensitivity of the silica-carbonate isotopic thermometer by a factor of 6 and that their results may therefore be invalid.

Shemesh *et al.* deduce the silica-carbonate fractionation curve by combining data from the silica-water fractionation and the carbonate-water fractionation. The latter can be found in studies by S. Epstein *et al.* (*2*) on biogenic calcite and by R. N. Clayton (*3*) on inorganically exchanged calcite. For biogenic silica, L. D. Labeyrie (*4*) showed that isotopic fractionation between biogenic silica and water follows closely the fractionation between crystalline quartz and water measured in higher temperature laboratory experiments (*5*). Similar agreement was found for amorphous silica precipitated in geothermal wells (*6*). The temperature dependence for deposition of silica by diatoms has been redetermined with the use of new analytical techniques (*7*), and results are in agreement with earlier findings, although the data are rather scattered.

Previous studies lead to the conclusion that quartz-calcite is a good approximation to diatom-foraminifera for the purposes of isotopic fractionation. The quartz-calcite isotopic fractionation is well known experimentally and theoretically at all temperatures (*8*). At ocean temperatures, the temperature coefficient of the quartz-calcite isotopic fractionation is −0.04 per mil per degrees Celsius. For an analytical precision of ±0.15 per mil, the paleotemperature